$CaTiO_3$-rich precipitates and their impacts on ferroelectric domains during heating in $(Ba,Ca)TiO_3$ ceramics

Odin Taylor,[a] Ethan Chaffee,[a] Xinchun Tian,[a] Changhao Zhao,[b,c] Lin Zhou,[a] and Xiaoli Tan[a,*]

[a]Department of Materials Science and Engineering, Iowa State University, Ames, Iowa 50011, U.S.A.

[b]Department of Materials and Earth Sciences, Technical University of Darmstadt, Darmstadt 64289, Germany

[c]State Key Laboratory of Electrical Insulation and Power Equipment, Xi'an Jiaotong University, Xi'an 710049, P. R. China

[*]Author to whom correspondence should be addressed: xtan@iastate.edu

ABSTRACT. Precipitates have been shown to harden bulk piezoelectric ceramics, manifested by their increased mechanical quality factor. In this work with a model system $(Ba,Ca)TiO_3$, we analyze the morphologies of $CaTiO_3$-rich precipitates and their impacts on the microstructures in their surrounding $BaTiO_3$-rich matrix. Also, the response of ferroelectric domains around $CaTiO_3$-rich precipitates during heating and cooling is observed *in-situ* with transmission electron microscopy. Domains attached to precipitates are observed remaining unchanged up to the Curie point at which they disappear. During cooling, domains are observed to form in the vicinity of precipitates and being held in place down to room temperature. Both observations corroborate previous findings that precipitates act as domain pinning points, behaving in a similar manner to earlier experiments with electrical field biasing. Dislocations are often seen around precipitates in the matrix grain and are observed interfering with domains during heating cycles. Dislocations may provide an additional mechanism to restrict domain wall motion and offer a greater piezoelectric hardening effect.

KEYWORDS: *In-situ* TEM, Precipitates, Dislocations, Piezoelectric Hardening, $(Ba,Ca)TiO_3$

1. INTRODUCTION

Many modern technologies rely on materials that exhibit the piezoelectric effect, a property that causes materials to deform when an electric field is applied to them or generate polarization with applied stress [1]. In order to suppress mechanisms that lead to energy loss, such as the motion of ferroelectric domain walls, piezoelectric materials are often "hardened" by introducing oxygen vacancies via acceptor doping, which impede domain wall motion [1,2]. Many piezoelectrics, including lead-based and lead-free materials, have been successfully hardened using this method [3-6].

However, a major issue with the traditional form of piezoelectric hardening using oxygen vacancies is a sensitivity to temperature and high vibration velocity [2,7]. At raised temperatures, oxygen vacancies become mobile and the internal bias field is disturbed, leading to deterioration of the hardening effect. This becomes an issue as demand for high-temperature piezoelectric devices increases [8]. Recently, higher-dimensional defects have been investigated in place of oxygen vacancies in order to reduce domain wall motion. Dislocations have been shown to be able to act as domain-pinning sites [9-11]. Volumetric defects, in the form of precipitates and intentional impurity particles, have also been proven to increase the mechanical quality factor [12-14], fulfilling the same purpose as oxygen vacancies. Volumetric defects can remain stable even at temperatures above the Curie point where piezoelectricity is lost. Studies have shown that volumetric defects and strain within a material can even increase the Curie point of piezoelectric materials [15]. Thus, they should be a much more effective and reliable way to harden piezoelectrics in high-power and high-temperature applications.

$BaTiO_3$ has been a useful model system in our previous *in-situ* transmission electron microscopy (TEM) work. In an undoped $BaTiO_3$ single crystal, we performed *in-situ* heating on specimens with dislocations [9]; while in polycrystalline ceramic samples with $CaTiO_3$-rich

precipitates, we carried out *in-situ* biasing experiments [16]. Both dislocations and precipitates were directly shown to exhibit pinning effects on ferroelectric domain walls. However, *in-situ* heating during TEM observation of $CaTiO_3$-rich precipitates in a $BaTiO_3$-rich matrix has not yet been documented.

To further the understanding of the effect the precipitates have on the $(Ba,Ca)TiO_3$ system and help expand the knowledge of precipitate interactions with domains in general, we conduct *in-situ* heating TEM experiments on the $(Ba,Ca)TiO_3$ ceramic in the present work. Precipitates are seen to cause an increased number of fine domains in the matrix around them, as well as to pin domains in place up to the Curie point. Precipitates are also observed to induce dislocations in the matrix, which in turn restrict domains as well. As such, precipitates demonstrate an added hardening effect through dislocations in materials like aged $(Ba,Ca)TiO_3$.

2. MATERIALS AND METHODS

Ceramic pellets of $(Ba,Ca)TiO_3$ with 20 wt.% $CaTiO_3$ were prepared as described in our previous work [12]. Pellets were quenched after sintering to avoid uncontrolled formation of precipitates during cooling. Samples were then aged at 1200-1300 ^oC for a number of hours to nucleate and grow $CaTiO_3$-rich precipitates. These samples were thinned to around 150 μm thickness and then ultrasonically cut into 3 mm diameter discs. After mechanical dimpling and a brief annealing at 200 ^oC, the discs were ion milled with Argon until perforation. The thin area around the perforation would be electron-transparent in TEM.

An FEI Tecnai G2-F20 TEM was used for chemical and microstructural analysis, as well as the *in-situ* heating experiments. Assisted by Kikuchi patterns, grains were aligned to low-index zone axes. Electron diffraction patterns were often taken of the $CaTiO_3$-rich precipitate particles, the surrounding $BaTiO_3$-rich matrix grain, or both. Energy-dispersive X-ray

spectroscopy (EDS) was utilized to confirm the composition of the matrix and precipitate. Heating experiments were performed by using a specialized heating TEM specimen holder (Model 652, Gatan). The temperature was first increased in steps until domains disappeared, then decreased back to room temperature before beginning another cycle. At each set temperature after image drift was at minimum, micrographs and diffraction patterns were recorded. Live videos of the heating/cooling process were also recorded.

3. RESULTS AND DISCUSSION

The microstructure and chemistry of a grain with a precipitate in (Ba,Ca)TiO_3 was first analyzed. As shown in Figure 1(a), a precipitate in a round shape was found within a grain, where the precipitate/matrix interface was highlighted by three bright curves. The selected area electron diffraction pattern (EDP) from the matrix grain indicates the $<112>_c$ zone-axis [Fig. 1(b), subscript c denotes pseudo-cubic notation]. According to the EDP, the inclined domain walls in Fig. 1(a) in the matrix grain are determined to be along the $\{\bar{1}01\}_c$ and $\{0\bar{1}1\}_c$ planes. In the imaged area, the large domains roughly along the horizontal direction are the $\{\bar{1}01\}_c$ domains and the fine domains in the lower-right part are the $\{0\bar{1}1\}_c$ ones. It appears that the precipitate partially blocks the top $\{\bar{1}01\}_c$ domain and completely stops the second $\{\bar{1}01\}_c$ domain in the left. EDS spectra were collected both on the precipitate and the matrix grain [Fig. 1(c)]. The results indicate that the precipitate is Ca-rich and Ba-poor while the matrix is Ba-rich and Ca-poor. In the previous work, we have confirmed that these Ca-rich precipitates are isostructural with $CaTiO_3$, with an orthorhombic perovskite structure at room temperature, while the matrix grain is $BaTiO_3$-rich perovskite with a tetragonal distortion [12].

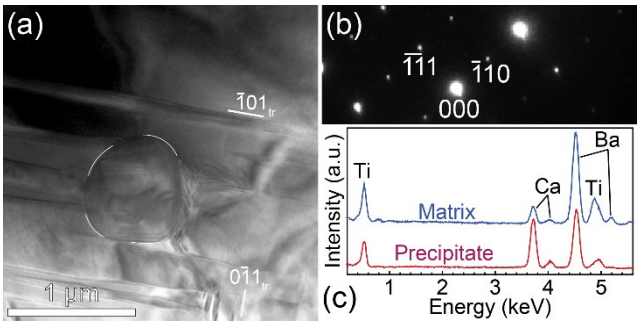

Fig. 1 (a) Bright-field TEM image of a precipitate (highlighted by curved lines) in a matrix grain. $\bar{1}01_{tr}$ and $0\bar{1}1_{tr}$ indicate the trace of the inclined $\{\bar{1}01\}_c$ and $\{0\bar{1}1\}_c$ planes on the specimen surface, respectively. (b) The $<112>_c$ zone-axis electron diffraction pattern recorded from the matrix grain. (c) EDS spectra of the matrix and the precipitate, showing large difference in Ca and Ba content.

The precipitate/matrix interfaces in aged samples often exhibit unique features. Figure 2(a) displays a large precipitate around 1.6 μm in size. This precipitate shows distinct facets along its edges; closer views are shown in the lower and right sections of (a) with higher magnification images of the boxed areas. Such features bear the growth mechanisms of the precipitates during aging and should be investigated in detail in future studies. Figure 2(b) shows another precipitate of ~0.6 μm in size with apparent facets. The EDP from the matrix grain is along the $<011>_c$ zone-axis. The large facet on the left side of the precipitate appears to be inclined to the electron beam and is close to the $\{\bar{1}01\}_c$ plane of the matrix grain. The impact of the precipitate on the surrounding matrix is obvious: It leads to the formation of a high density of fine domains around it, corroborating our previous observations [12]. According to the EDP, the domain walls (inclined to the electron beam) are likely on the $\{\bar{1}01\}_c$ and $\{101\}_c$ planes.

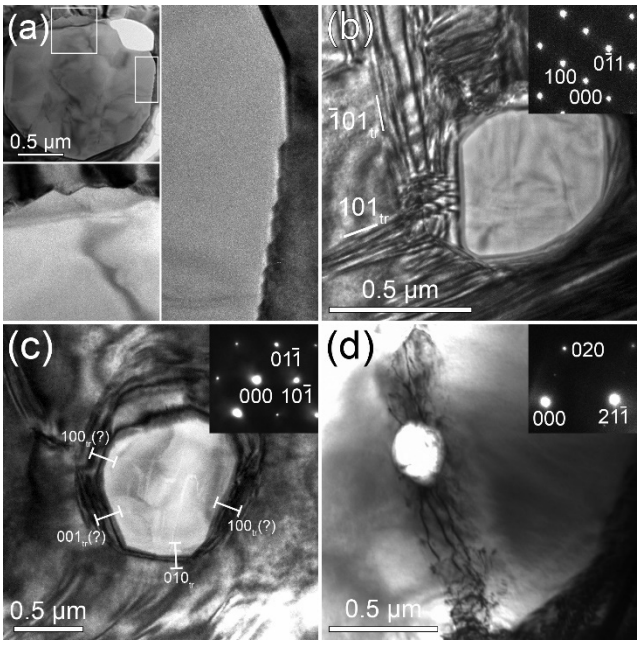

Fig. 2 Various $CaTiO_3$-rich precipitates and their impact on the surrounding matrix. Subscript tr denotes the trace of the inclined planes on the specimen surface. (a) Facets and terraces on the precipitate/matrix interface. The two boxed areas are zoomed in on the lower and the right parts. (b) Bright-field image of high-density fine domains around a precipitate, with domain walls likely along the $\{\bar{1}01\}_c$ and $\{101\}_c$ planes. The inset shows the $<011>_c$ zone-axis EDP from the matrix. (c) Another precipitate with facets. The inset displays the $<111>_c$ zone-axis EDP from the matrix. The features below the precipitate are likely to be dislocations. (d) Bright field image of dislocations around a likely precipitate. The inset shows the $<102>_c$ zone-axis EDP from the matrix.

Figure 2(c) shows another precipitate around 1.0 μm in size. The dark lines curving towards the left below the precipitate, as well as the line jutting off its left side, are likely to be dislocations rather than domain walls. It should be note that dislocations are line defects, are often wavy/curved in their appearance, and remain even when heated to above the Curie temperature. On the other hand, domain walls are planar defects, most often are straight, appear in pairs, and vanish when heated to above the Curie temperature. Thus, they can be distinguished

by changing the tilting conditions and/or heating the specimen in TEM. The grain was imaged along its $<111>_c$ zone-axis. Based on the EDP of the matrix grain, the major facets of the precipitate appear to be on the $\{010\}_c$ plane family of the matrix grain, which is consistent with our previous work [16]. However, there exists uncertainty in assigning 100_{tr} and 001_{tr} in Fig. 2(c) given the limited information, as $\{\bar{2}23\}_c$ and $\{32\bar{2}\}_c$ also have close traces on the specimen surface. Figure 2(d) displays a grain oriented along its $<102>_c$ zone-axis. There is a pore of around 0.3 μm in size within the grain, which is highly likely caused by the loss of a $CaTiO_3$-rich precipitate during the ion milling process. A band of dislocations can be clearly seen above and below the pore (precipitate), extending throughout the grain.

In-situ heating TEM experiments were conducted on aged specimens. The results from one grain are displayed in Figure 3. According to the EDPs shown in Fig. 3(c) and (d), it is interesting to notice that both the matrix and the precipitate are oriented along their $<011>_c$ zone-axis. However, the precipitate appears to be rotated 30° clockwise with respect to the matrix. Such a large orientation difference between the precipitate and the matrix appears to be common in the $(Ba,Ca)TiO_3$ ceramic [16]. The interfaces appear to be incoherent and non-epitaxial. According to the EDP of the matrix, the facets of the precipitate appear to be along the $\{100\}_c$, $\{2\bar{1}1\}_c$, $\{\bar{1}\bar{1}1\}_c$, and $\{1\bar{1}1\}_c$ planes, as marked in Fig. 3(a). It should be noted that the contrast within the $CaTiO_3$-rich precipitate is presumably indicative of ferroelastic domains. The domains in the matrix grain, indexed with $\{101\}_c$ and $\{110\}_c$ domain walls in Fig. 3(a), are ferroelectric domains, some of which are observed terminating at the precipitate interface.

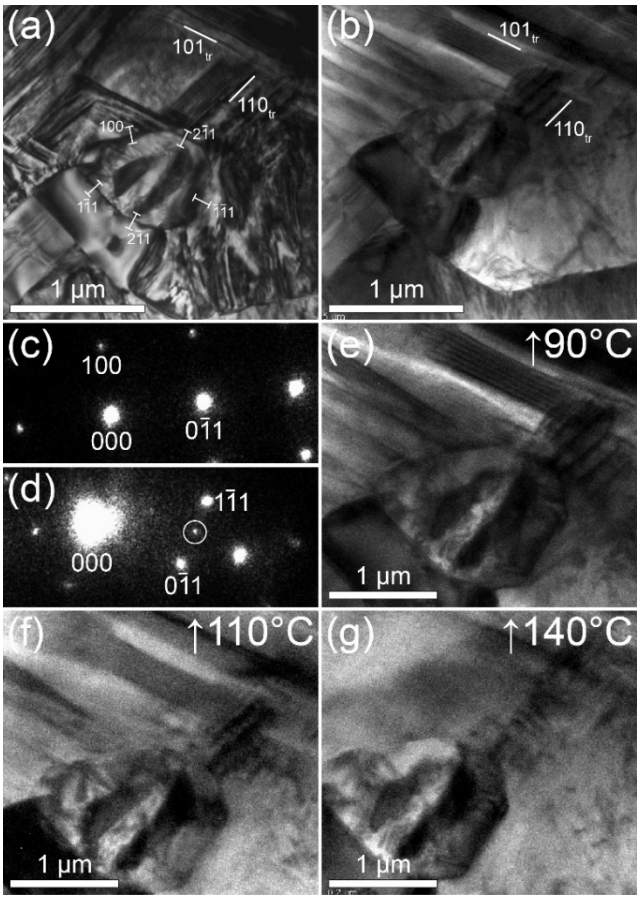

Fig. 3 *In-situ* heating TEM of the $(Ba,Ca)TiO_3$ ceramic. Subscript tr indicates the trace of the indexed plane on the specimen surface. (a) Bright field micrograph of a grain with a $CaTiO_3$-rich precipitate in the center. The facets of the precipitate appear to be edge-on and are indexed according to the EDP of the matrix. (b) The same area at room temperature after two heating/cooling cycles. (c, d) EDPs of the matrix and the precipitate, both on the $<011>_c$ zone-axis. One superlattice spot in the precipitate EDP is highlighted by a circle. (e-g) *In-situ* heating of specimen up to above the Curie point, with corresponding temperatures estimated from the recorded video.

The heating experiment involved screen recording of short-time frames while the sample was heated. Due to the nature of the electron-transparent specimen, the Curie point will not

exactly line up with the expected value of 116 °C for $(Ba,Ca)TiO_3$ [17]. However, the point at which domains disappear from the material (indicating a phase transition) remains obvious. The specimen first underwent two heating/cooling cycles to test if the ferroelectric domains in the matrix were responsive to temperature changes. After these two thermal cycles, the domain arrangement in the matrix changed, as shown in Fig. 3(b), with the $\{101\}_c$ set of domains dominant. The microstructure evolution during the subsequent heating was then recorded in a video file and representative micrographs were extracted from the video file. The temperatures at each micrograph in Fig. 3(e-g) are estimated and the actual temperature is expected to be within ±10 °C of the marked temperature. It is found that the domains in the matrix are largely unchanged at temperatures up to 90 °C [Fig. 3(e)]. At 110 °C [Fig. 3(f)], the domains begin to taper away from the precipitates, losing their attachment to it. At 140 °C [Fig. 3(g)], all the $\{101\}_c$ domains around the precipitate disappear. Only some remnants of the $\{110\}_c$ domains are barely seen in the upper right area. All the domains in the matrix completely disappear upon further increase in temperature (not shown here).

The results of the *in-situ* TEM experiments on another specimen are shown in Figure 4. A grain with a precipitate was located and imaged, with visible fine domains around the precipitate [Fig. 4(a)]. A selected area EDP, taken from the precipitate along its $<111>_c$ zone-axis, is displayed in Fig. 4(b). Three sets of superlattice spots are visible, with $½\{01\bar{1}\}_c$, $½\{10\bar{1}\}_c$, and $½\{1\bar{1}0\}_c$ highlighted by circles in Fig. 4(b). Their presence is in support of the orthorhombic perovskite structure of the precipitate [18] and indicates that the selected area in this precipitate particle contains multiple ferroelastic domains. In addition, dislocations are visible in both the precipitate and the matrix (highlighted by the short arrow in upper left of the micrograph).

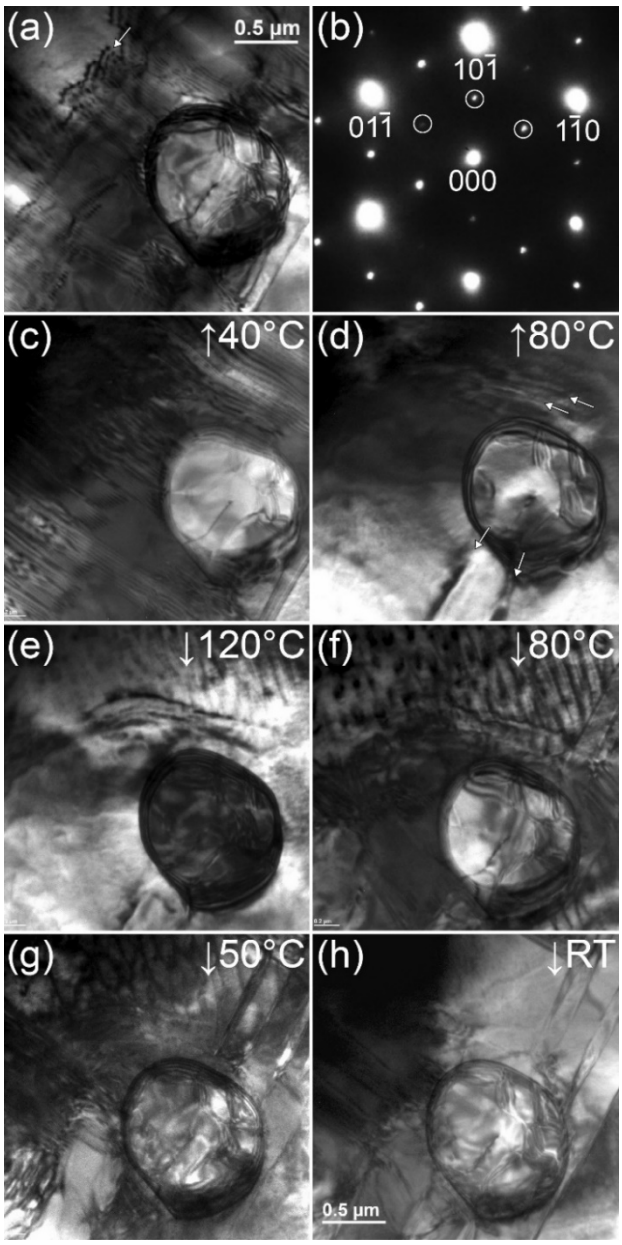

Fig. 4 *In-situ* heating/cooling TEM observation on the domains surrounding a precipitate. (a) Bright field micrograph of the precipitate and surrounding ferroelectric domains. (b) Selected-area EDP within the precipitate along its $<111>_c$ zone-axis with circled superlattice spots. (c-d) Heating of the specimen, showing disappearance of ferroelectric domains in the matrix grain. (e-h) Cooling of the specimen down to room temperature (RT), showing reformation of ferroelectric domains in the matrix pinned to both the precipitate and the dislocation above it. The short arrows in (a) and (d) denote dislocations.

This specimen was subjected to heating and cooling experiments in a stepwise manner to set temperatures. During heating, the domain structure in the matrix grain remains largely unchanged up to 40 °C [Fig. 4(c)], and most domains vanish at or slightly above 80 °C [Fig. 4(d)]. Figure 4(d) also reveals curved dislocations above the precipitate as well as dislocations extending from below it (noted with bright short arrows). These dislocations, and other microstructures in the matrix grain, did not change even when the specimen was heated up to and beyond 360 °C (not pictured). During cooling, domains start to form at 120 °C [Fig. 4(e)], first appearing blocked by the dislocations above the precipitate. Figure 4(f) shows the specimen at 80 °C, displaying increased domain formation activity all around the precipitate. Specifically, a wide domain can be seen terminating at the precipitate in the top right of the image. The domain structure drastically changes again at 50 °C [Fig. 4(g)], with new domains terminating on the left side of the precipitate, and domain morphology changing throughout the rest of the image. At room temperature [Fig. 4(h)], only a few domains remain in the image, most of which are affixed to the precipitate. The fine domains blocked by the dislocations appear to have merged into a large one.

The ferroelastic domain structure within the $CaTiO_3$-rich precipitate also shows changes during the heating and cooling process, likely to accommodate thermal stresses during temperature variation [Fig. 4(c-g)]. After the heating/cooling cycle at room temperature, the ferroelastic domains appear to have reverted back to a similar state [compare Fig. 4(a) to (h)].

The observation that $CaTiO_3$-rich precipitates induce high density fine domains in their vicinity is consistent with our previous work [12]. Interestingly, dislocations are frequently seen around precipitates [Fig. 2(c) and (d), Fig. 4(d)], likely due to thermal stresses during cooling

after the aging process. Distinct facets and terraces are also observed on the boundary between the precipitate and the matrix, which are consistent with previous observations [16].

A pinning effect is observed during the heating of both specimens. During heating [Fig. 3(e-g), Fig. 4(c-d)], domains that terminate at precipitates do not appear to change shape until disappearing (at the Curie point). Additionally, $CaTiO_3$-rich precipitates do appear stable and unchanging up to high temperatures, with only their internal ferroelastic domain structure changing slightly. A similar ferroelectric domain pinning effect with both precipitates and dislocations is observed during cooling [Fig. 4(e-h)]. Many domains form at just below the Curie point [Fig. 4(e)] terminating at a dislocation. During the later portion of cooling, domains form and terminate at the precipitate. Once cooled to room temperature, domains that were pinned at the precipitate at their formation remained in place, whereas the rest of the domains within the grain appeared to rearrange into a coarser structure. Both of these pinning effects are similar to the observations when applying electric field to specimens of the same composition, with domains affixed to precipitates maintaining their form up to field saturation and forming stable morphologies with precipitates early in the decreasing of electric field from saturation [16].

Dislocations are frequently observed around precipitates and they exhibit a blocking effect on domain growth in the $(Ba,Ca)TiO_3$ ceramic as in $BaTiO_3$ single crystal [9]. This implies that precipitates may cause an additional hardening effect to piezoelectrics with their induced dislocations, as dislocations have been shown to interact strongly with ferroelectric domains [9-11].

4. CONCLUSIONS

Using (Ba,Ca)TiO_3 as a model system, the $CaTiO_3$-rich precipitates and their interactions with ferroelectric domains in the $BaTiO_3$-rich matrix under heating and cooling are examined. Precipitates are observed to have distinct facets and terraces; they often cause the formation of dislocations as well as fine domains around themselves in the matrix grain. During heating, domains affixed to precipitates do not change form until they disappear above the Curie point. Additionally, precipitates remain stable and unchanging to high temperatures. During cooling, ferroelectric domains formed just below the Curie point, which terminate at the precipitate, remain in the same configuration until room temperature. This provides evidence for the hardening effect of precipitates through stabilizing the morphology of nearby domains. Furthermore, the strong interactions of dislocations (induced by precipitates) with domain growth enhance the precipitate hardening effect.

5. REFERENCES

[1] B. Jaffe, W. R. Cook, H. L. Jaffe, *Piezoelectric Ceramics* (Academic Press, 1971).

[2] K. Uchino, J. H. Zheng, Y. H. Chen, X. H. Du, J. Ryu, Y. Gao, S. Ural, S. Priya, S. Hirose, Loss mechanisms and high power piezoelectrics. J. Mater. Sci. **41**, 217 (2006). https://doi.org/10.1007/s10853-005-7201-0

[3] R. Zuo, J. Fu, S. Su, X. Fang, J. L. Cao, Electrical properties of manganese modified sodium potassium lithium niobate lead-free piezoelectric ceramics. J. Mater. Sci: Mater. Electron. **20**, 212 (2009). https://doi.org/10.1007/s10854-008-9701-6

[4] H. J. Lee, S. O. Ural, L. Chen, K. Uchino, S. Zhang, High power characteristics of lead-free piezoelectric ceramics. J. Am. Ceram. Soc. **95**, 3383 (2012). https://doi.org/10.1111/j.1551-2916.2012.05462.x

[5] D. Wang, Y. Liao, Z. Peng, Q. Zheng, X. Wei, T. Wang, D. Lin, Defect-relevant piezoelectric and ferroelectric properties in $LiCuTa_3O_9$-doped $K_{0.5}Na_{0.5}NbO_3$ lead-free piezoceramics. J. Mater. Sci.: Mater. Electron. **30**, 2563 (2019). https://doi.org/10.1007/s10854-018-0531-x

[6] S. Samanta, S. Venkataraman, K. Sethupathi, Effect of Nb and Fe co-doping on microstructure, dielectric response, ferroelectricity and energy storage density of PLZT. J. Mater. Sci.: Mater. Electron. **29**, 20383 (2018). https://doi.org/10.1007/s10854-018-0173-z

[7] M. Li, M. J. Pietrowski, R. A. De Souza, H. Zhang, I. M. Reaney, S. N. Cook, J. A. Kilner, D. C. Sinclair, A family of oxide ion conductors based on the ferroelectric perovskite $Na_{0.5}Bi_{0.5}TIO_3$. Nat. Mater. **13**, 31 (2014). https://doi.org/10.1038/nmat3782

[8] T. Stevenson, D. G. Martin, P. I. Cowin, A. Blumfield, A. J. Bell, T. P. Comyn, P. M. Weaver, Piezoelectric materials for high temperature transducers and actuators. J. Mater. Sci: Mater. Electron **26**, 9256 (2015). https://doi.org/10.1007/s10854-015-3629-4

[9] M. Höfling, X. Zhou, L. M. Riemer, E. Bruder, B. Liu, L. Zhou, P. B. Groszewicz, F. Zhuo, B.-X. Xu, K. Durst, X. Tan, D. Damjanovic, J. Koruza, J. Rödel, Control of polarization in bulk ferroelectrics by mechanical dislocation imprint. Science **372**, 961 (2021). https://doi.org/10.1126/science.abe3810

[10] G. Deguchi, R. Kobayashi, H. Azuma, S. Ogata, M. Uranagase, S. Spreafico, Asymmetric domain nucleation from dislocation core in barium titanate: molecular dynamics simulation using machine-learning potential through active learning. Phys. Status Solidi – Rapid Res. Lett. 2300292 (2023). https://doi.org/10.1002/pssr.202300292

[11] X. Zhou, Z. Liu, B.-X. Xu, Influence of dislocations on domain walls in perovskite ferroelectrics: Phase-field simulation and driving force calculation. Int. J. Solids Str. **238**, 111391 (2022). https://doi.org/10.1016/j.ijsolstr.2021.111391

[12] C. Zhao, S. Gao, T. Yang, M. Scherer, J. Schultheiß, D. Meier, X. Tan, H.-J. Kleebe, L.-Q. Chen, J. Koruza, J. Rödel, Precipitation hardening in ferroelectric ceramics. Adv. Mater. **33**, 2102421 (2021). https://doi.org/adma.202102421

[13] H. Li, H. Chen, X. Li, J. Xing, W. Liu, Z. Tan, M. Mo, N. Chen, M. Tang, J. Zhu, Hardening effect on the electromechanical properties of KNN-based ceramics using a composite approach, ACS Appl. Mater. Interf. **15**, 36576 (2023). https://doi.org/10.1021/acsami.3c06770

[14] G. Wang, P. Ren, P. Zhang, C. Guo, F. Zhuo, Z. Liu, Electromechanical hardening of $Na_{1/2}Bi_{1/2}TiO_3$-based ceramics by the *in-situ* formed secondary phase, Ceram. Int. **50**, 18227 (2024). https://doi.org/10.1016/j.ceramint.2024.02.307

[15] J. Li, Microstructure and piezoelectric properties of lead zirconate titanate nanocomposites reinforced with *in-situ* formed ZrO_2 nanoparticles. Materials **15**, 1389 (2022). https://doi.org/10.3390/ma15041389

[16] O. Taylor, E. Chaffee, B. Liu, C. Zhao, J. Rödel, L. Zhou, X. Tan, Electric field response of ferroelectric domains near non-polar precipitates in $BaTiO_3$-based ceramics. Appl. Phys. Lett. **124**, 212904 (2024). https://doi.org/10.1063/5.0211248

[17] K. Feliksik, L. Kozielski, I. Szafraniak-Wiza, T. Goryczka, M. Adamczyk-Habrajska, Dielectric and impedance studies of (Ba,Ca)TiO_3 ceramics obtained from mechanically synthesized powders. Materials **12**, 4036 (2019). https://doi.org/10.3390/ma12244036

[18] D. I. Woodward, I. M. Reaney, Electron diffraction of tilted perovskites, Acta Crystallogr. B: Struct. Sci. **61**, 387 (2005). https://doi.org/10.1107/S0108768105015521

6. STATEMENTS AND DECLARATIONS

FUNDING

This work was supported by the USA National Science Foundation (NSF) through Grant No. DMR-2110264.

COMPETING INTERESTS

The authors have no conflicts of interest to disclose.

AUTHOR CONTRIBUTIONS

Odin Taylor: Data curation; Formal analysis; Visualization; Writing – original draft.

Ethan Chaffee: Data curation; Methodology; Validation.

Xinchun Tian: Data curation; Methodology.

Changhao Zhao: Investigation; Writing – review & editing.

Lin Zhou: Conceptualization; Funding acquisition; Supervision; Writing – review & editing.

Xiaoli Tan: Conceptualization; Funding acquisition; Project administration; Supervision; Writing – original draft, review & editing

DATA AVAILABILITY

The data that support the findings of this study are available from the corresponding authors upon reasonable request.